Is Using A Complex Control Gain in Three-phase FLLs Reasonable?

Golestan, S.; Guerrero, J. M.; Vasquez, J. C.

Published in:
IEEE Transactions on Industrial Electronics

DOI (link to publication from Publisher):
10.1109/TIE.2019.2903748

Publication date:
2020

Document Version
Accepted author manuscript, peer reviewed version

This article has been accepted for publication in a future issue of this journal, but has not been fully edited. Content may change prior to final publication. Citation information: DOI 10.1109/TIE.2019.2903748, IEEE Transactions on Industrial Electronics

Is Using A Complex Control Gain in Three-phase FLLs Reasonable?

Saeed Golestan, *Senior Member, IEEE*, Josep M. Guerrero, *Fellow, IEEE*, and Juan C. Vasquez, *Senior Member, IEEE*

***Abstract*—A frequency-locked loop (FLL) is a stationary reference frame adaptive recursive filter with a high popularity in different engineering applications, particularly for extracting the grid voltage parameters and synchronization of power converters. In three-phase applications, the reduced-order generalized integrator-based FLL (ROGI-FLL) is a standard structure and a basic unit for designing more advanced FLLs. Very recently, to supposedly enhance the ROGI-FLL performance, using a complex control gain (instead of the traditional real one) in its structure has been proposed in the literature. Applying such a control gain, however, has some drawbacks that have not been discussed before. Explaining these shortcomings is the main objective of this work. To facilitate this task, a small-signal model for a basic complex-coefficient ROGI-FLL (CC-ROGI-FLL) is obtained and analyzed. A numerical performance comparison between the CC-ROGI-FLL and ROGI-FLL is also conducted.**

***Index Terms*—Complex-coefficient filter, frequency-locked loop (FLL), reduced-order generalized integrator (ROGI), synchronization, three-phase systems.**

I. Introduction

FREQUENCY-LOCKED loop (FLL), which can be understood as a stationary reference frame adaptive recursive filter, has received much attention in different engineering applications, particularly in power and energy areas for the synchronization of power converters, decomposition of power signals, control of electrical motors, etc. [1]–[10].

Implementing FLLs in three-phase applications, which this work focuses on, is often carried out using a reduced-order generalized integrator (ROGI) [1]–[3]. The block diagram of a standard ROGI-FLL, also known as the complex bandpass filter-based FLL (CBF-FLL), can be observed in Fig. 1. A key element in this structure is a first-order CBF, which is realized by using a ROGI centered at the fundamental frequency in a unity feedback control loop. This CBF extracts the grid voltage fundamental component. The frequency estimator also plays an important role in the ROGI-FLL structure as it extracts the grid frequency and adapts the ROGI center frequency to the frequency changes.

In recent years, some research works for designing more advanced three-phase FLLs have been done. For example, to enhance the ROGI-FLL filtering capability, employing one or more ROGIs centered at concerned disturbance frequencies in parallel with the main ROGI, which is centered at the fundamental frequency, is proposed in [1]–[3]. In [4], the concept of in-loop filter for designing three-phase FLLs with a high filtering capability is introduced. According to this concept, the standard ROGI-FLL disturbance rejection capability can be considerably enhanced by including a band-pass-like filter with the center frequency at the fundamental frequency in its control loop. In [5], using one or more first-order CBFs as the prefiltering stage of the ROGI-FLL (it is called the CBF-FLL in [5]) is proposed. These CBFs are adapted to frequency changes using a frequency feedback loop.

Very Recently, to enhance the ROGI-FLL performance, using a complex control gain (which is implemented through a

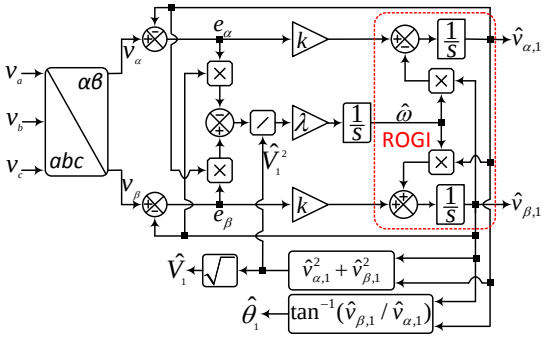

Fig. 1. Block diagram of the standard ROGI-FLL. v_a, v_b, and v_c are the three-phase input signals. v_α and v_β are the $\alpha\beta$-axis input signals, and $\hat{v}_{\alpha,1}$ and $\hat{v}_{\beta,1}$ are estimates of their fundamental components. $\hat{V}_1$, $\hat{\theta}_1$, and $\hat{\omega}$ represent estimates of the amplitude, phase angle, and frequency of the input signal fundamental component, respectively. k and λ are the ROGI-FLL control parameters.

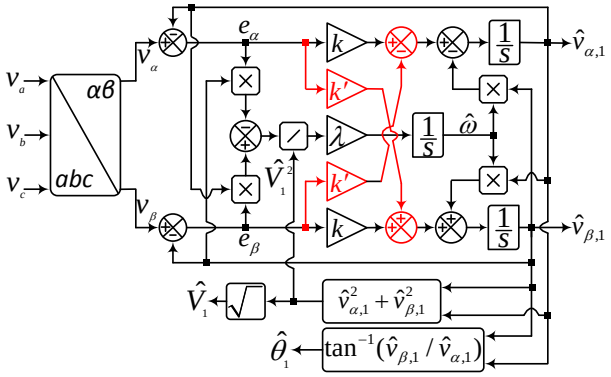

Fig. 2. Block diagram of the CC-ROGI-FLL. k' is an additional degree freedom (control gain). The definition of other parameters can be found in the caption of Fig. 1.

Authors are with the Department of Energy Technology, Aalborg University, Aalborg DK-9220, Denmark (e-mail: sgd@et.aau.dk; joz@et.aau.dk; juq@et.aau.dk).

Color versions of one or more of the figures in this paper are available online at http://ieeexplore.ieee.org.

cross-coupling between the α- and β-axis) in its structure has been proposed in [9]. Fig. 2 illustrates the resultant structure, which is here briefly referred to as the complex-coefficient ROGI-FLL (CC-ROGI-FLL).[1] Based on some numerical results, it is claimed in [9] that using a complex control gain results in a better compromise between the speed and damping of the FLL transient response and, therefore, provides a faster dynamic behavior with a much lower overshoot. Regardless of some exaggerations in this claim, it is demonstrated here that using a complex control gain in three-phase FLLs has some serious drawbacks that have been neglected in [9]. Creating a strong coupling between the phase/frequency and amplitude estimation loops, complicating the analysis and tuning procedure, and amplifying frequency components in the neighborhood of the fundamental frequency are notable examples of these shortcomings. To facilitate understanding of these problems, a small-signal model for the CC-ROGI-FLL is derived, and some numerical results are presented.

II. Modeling

To facilitate the analysis of the CC-ROGI-FLL, its small-signal modeling is presented in this section. To this end, some assumptions, definitions, and basic equations describing the CC-ROGI-FLL dynamics are presented first.

A. Assumptions, Definitions, and Basic Equations

It is assumed that the three-phase input signals of the CC-ROGI-FLL are without any distortion. Therefore, its $\alpha\beta$-axis input and output signals can be considered as

$$\begin{aligned} v_\alpha &= V_1 \cos(\theta_1) \\ v_\beta &= V_1 \sin(\theta_1) \end{aligned} \tag{1}$$

$$\begin{aligned} \hat{v}_{\alpha,1} &= \hat{V}_1 \cos(\hat{\theta}_1) \\ \hat{v}_{\beta,1} &= V_1 \sin(\hat{\theta}_1) \end{aligned} \tag{2}$$

where V_1 and θ_1 denote the amplitude and phase angle of the grid voltage fundamental component, respectively, and $\hat{V}_1$ and $\hat{\theta}_1$, as defined before, are estimations of these parameters. It is assumed that the actual and estimated quantities are very close to each other.

The following definitions are also made for the small-signal modeling of the CC-ROGI-FLL, in which the subscript n denotes the nominal value and Δ denotes a small perturbation.

$$\begin{aligned} \omega &= \omega_n + \Delta\omega \\ V_1 &= V_n + \Delta V_1 \\ \theta_1 &= \theta_n + \Delta\theta_1 \\ \hat{\omega} &= \omega_n + \Delta\hat{\omega} \\ \hat{V}_1 &= V_n + \Delta\hat{V}_1 \\ \hat{\theta}_1 &= \theta_n + \Delta\hat{\theta}_1 \end{aligned} \tag{3}$$

[1]It is called the complex-coefficient complex-variable filter (CC-CVF) in [9].

The following equations, which describe the CC-ROGI-FLL dynamics, may also be easily obtained from Fig. 2.

$$\frac{d\hat{v}_{\alpha,1}}{dt} = -\hat{\omega}\hat{v}_{\beta,1} + k(v_\alpha - \hat{v}_{\alpha,1}) - k'(v_\beta - \hat{v}_{\beta,1}) \tag{4}$$

$$\frac{d\hat{v}_{\beta,1}}{dt} = \hat{\omega}\hat{v}_{\alpha,1} + k(v_\beta - \hat{v}_{\beta,1}) + k'(v_\alpha - \hat{v}_{\alpha,1}) \tag{5}$$

$$\begin{aligned} \frac{d\hat{\omega}}{dt} &= \frac{\lambda}{\hat{V}_1^2}\left[\hat{v}_{\alpha,1}(v_\beta - \hat{v}_{\beta,1}) - \hat{v}_{\beta,1}(v_\alpha - \hat{v}_{\alpha,1})\right] \\ &= \frac{\lambda}{\hat{V}_1^2}\left[\hat{v}_{\alpha,1}v_\beta - \hat{v}_{\beta,1}v_\alpha\right] \end{aligned} \tag{6}$$

$$\hat{\theta}_1 = \tan^{-1}\left(\hat{v}_{\beta,1}/\hat{v}_{\alpha,1}\right) \tag{7}$$

$$\hat{V}_1 = \sqrt{\hat{v}_{\alpha,1}^2 + \hat{v}_{\beta,1}^2} \tag{8}$$

B. Modeling Procedure

The modeling of the CC-ROGI-FLL is divided into three distinct stages. A complete model is finally obtained using the results of these stages.

1) Frequency Estimation: Substituting (1) and (2) into (6) yields

$$\begin{aligned} \frac{d\hat{\omega}}{dt} &= \frac{\lambda V_1 \hat{V}_1}{\hat{V}_1^2}\overbrace{\left[\cos(\hat{\theta}_1)\sin(\theta_1) - \sin(\hat{\theta}_1)\cos(\theta_1)\right]}^{\sin(\theta_1 - \hat{\theta}_1)} \\ &= \frac{\lambda V_1}{\hat{V}_1}\sin(\theta_1 - \hat{\theta}_1). \end{aligned} \tag{9}$$

As we have already assumed that $\hat{\theta}_1 \approx \theta_1$ and $\hat{V}_1 \approx V_1$, (9) can be approximated by

$$\frac{d\hat{\omega}}{dt} \approx \lambda(\theta_1 - \hat{\theta}_1). \tag{10}$$

Considering the definitions (3), (10) can be rewritten as

$$\frac{d\Delta\hat{\omega}}{dt} \approx \lambda(\Delta\theta_1 - \Delta\hat{\theta}_1). \tag{11}$$

2) Phase Estimation: Differentiating (7) with respect to time yields

$$\frac{d\hat{\theta}_1}{dt} = \frac{\hat{v}_{\alpha,1}\frac{d\hat{v}_{\beta,1}}{dt} - \hat{v}_{\beta,1}\frac{d\hat{v}_{\alpha,1}}{dt}}{\hat{v}_{\alpha,1}^2 + \hat{v}_{\beta,1}^2} = \frac{\hat{v}_{\alpha,1}\frac{d\hat{v}_{\beta,1}}{dt} - \hat{v}_{\beta,1}\frac{d\hat{v}_{\alpha,1}}{dt}}{\hat{V}_1^2}. \tag{12}$$

Substituting (4) and (5) into (12) gives (13) at the bottom of the page. Considering (1) and (2), (13) can be rewritten as

$$\begin{aligned} \frac{d\hat{\theta}_1}{dt} &= \hat{\omega} + \frac{k}{\lambda}\frac{d\hat{\omega}}{dt} + \frac{k'}{\hat{V}_1^2}\left[V_1\hat{V}_1\cos(\theta_1 - \hat{\theta}_1) - \hat{V}_1^2\right] \\ &\approx \hat{\omega} + \frac{k}{\lambda}\frac{d\hat{\omega}}{dt} + \frac{k'}{\hat{V}_1}\left[V_1 - \hat{V}_1\right]. \end{aligned} \tag{14}$$

$$\frac{d\hat{\theta}_1}{dt} = \frac{\hat{\omega}\overbrace{\left[\hat{v}_{\alpha,1}^2 + \hat{v}_{\beta,1}^2\right]}^{\hat{V}_1^2} + k\overbrace{\left[\hat{v}_{\alpha,1}(v_\beta - \hat{v}_{\beta,1}) - \hat{v}_{\beta,1}(v_\alpha - \hat{v}_{\alpha,1})\right]}^{\left(\hat{V}_1^2/\lambda\right)\frac{d\hat{\omega}}{dt}} + k'\left[\hat{v}_{\alpha,1}(v_\alpha - \hat{v}_{\alpha,1}) + \hat{v}_{\beta,1}(v_\beta - \hat{v}_{\beta,1})\right]}{\hat{V}_1^2} \tag{13}$$

This article has been accepted for publication in a future issue of this journal, but has not been fully edited. Content may change prior to final publication. Citation information: DOI 10.1109/TIE.2019.2903748, IEEE Transactions on Industrial Electronics

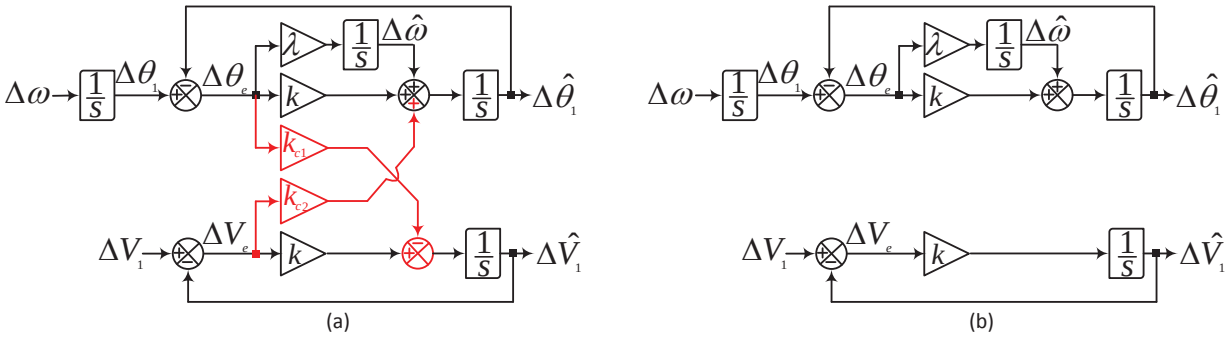

Fig. 3. (a) Small-signal model of the CC-ROGI-FLL. (b) Small-signal model of the ROGI-FLL. $k_{c1} = V_n k'$ and $k_{c2} = k'/V_n$. V_n is the nominal amplitude.

Using the definitions (3), (14) can be rewritten as

$$\frac{d\Delta\hat{\theta}_1}{dt} \approx \Delta\hat{\omega} + \frac{k}{\lambda}\frac{d\Delta\hat{\omega}}{dt} + \frac{k'}{V_n}\left[\Delta V_1 - \Delta\hat{V}_1\right]. \tag{15}$$

3) Amplitude Estimation: Differentiating (8) with respect to time yields

$$\frac{d\hat{V}_1}{dt} = \frac{\hat{v}_{\alpha,1}\frac{d\hat{v}_{\alpha,1}}{dt} + \hat{v}_{\beta,1}\frac{d\hat{v}_{\beta,1}}{dt}}{\hat{V}_1}. \tag{16}$$

Substituting (4) and (5) into (16) gives (17) at the bottom of the page, which can be approximated by (18) by considering (1) and (2).

$$\begin{aligned}\frac{d\hat{V}_1}{dt} &= -\frac{k'\hat{V}_1}{\lambda}\frac{d\hat{\omega}}{dt} + \frac{k}{\hat{V}_1}\left[V_1\hat{V}_1\cos(\theta_1 - \hat{\theta}_1) - \hat{V}_1^2\right] \\ &\approx -\frac{k'\hat{V}_1}{\lambda}\frac{d\hat{\omega}}{dt} + k\left[V_1 - \hat{V}_1\right]\end{aligned} \tag{18}$$

Using (10) and the definitions (3), (18) can be rewritten as

$$\frac{d\Delta\hat{V}_1}{dt} \approx -k'V_n\left[\Delta\theta_1 - \Delta\hat{\theta}_1\right] + k\left[\Delta V_1 - \Delta\hat{V}_1\right]. \tag{19}$$

4) Complete Model: Equations (11), (15), and (19) are three first-order differential equations that describe the dynamics of the CC-ROGI-FLL in estimating the frequency, phase angle, and amplitude of the fundamental component of its input. Using these differential equations, the complete small-signal model of the CC-ROGI-FLL can be derived as depicted in Fig. 3(a).

To evaluate the model accuracy, a 20° phase jump test is conducted in the Matlab/Simulink environment, and the results of the CC-ROGI-FLL are compared with those predicted by its model. Fig. 4 shows the results of this assessment. We can observe that the model demonstrates quite high accuracy. The small differences between the actual and predicted results are because of the approximations made during the modeling procedure.

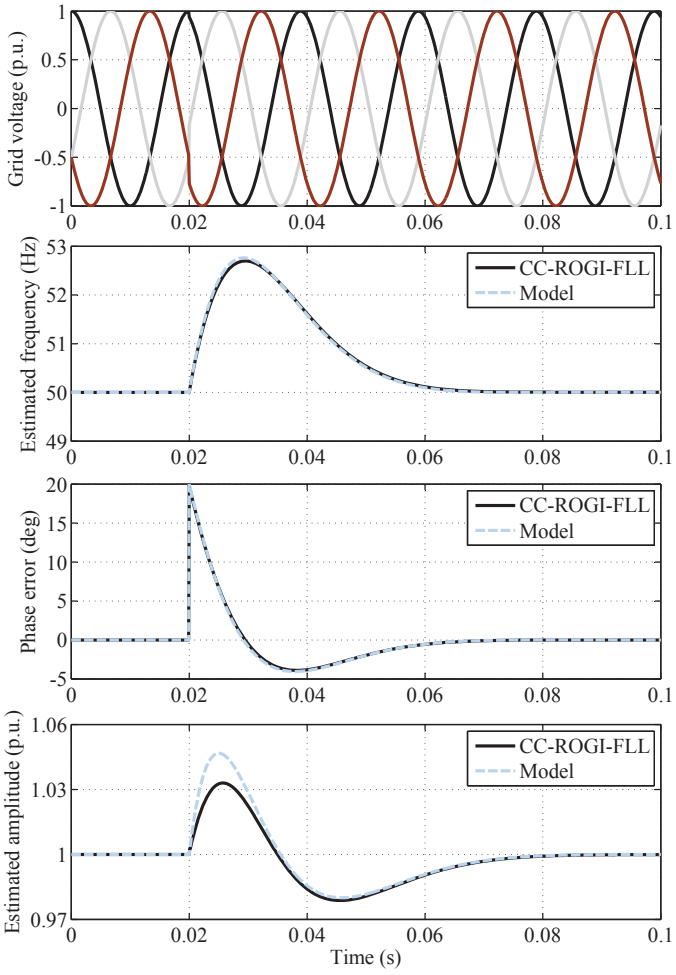

Fig. 4. Model accuracy assessment. Control parameters: $k = 160$, $k' = -64$, and $\lambda = 12791$. The sampling frequency throughout this work is 10 kHz.

$$\frac{d\hat{V}_1}{dt} = \frac{-k'\overbrace{\left[\hat{v}_{\alpha,1}(v_\beta - \hat{v}_{\beta,1}) - \hat{v}_{\beta,1}(v_\alpha - \hat{v}_{\alpha,1})\right]}^{(\hat{V}_1^2/\lambda)\frac{d\hat{\omega}}{dt}} + k\left[\hat{v}_{\alpha,1}(v_\alpha - \hat{v}_{\alpha,1}) + \hat{v}_{\beta,1}(v_\beta - \hat{v}_{\beta,1})\right]}{\hat{V}_1} \tag{17}$$

This article has been accepted for publication in a future issue of this journal, but has not been fully edited. Content may change prior to final publication. Citation information: DOI 10.1109/TIE.2019.2903748, IEEE Transactions on Industrial Electronics

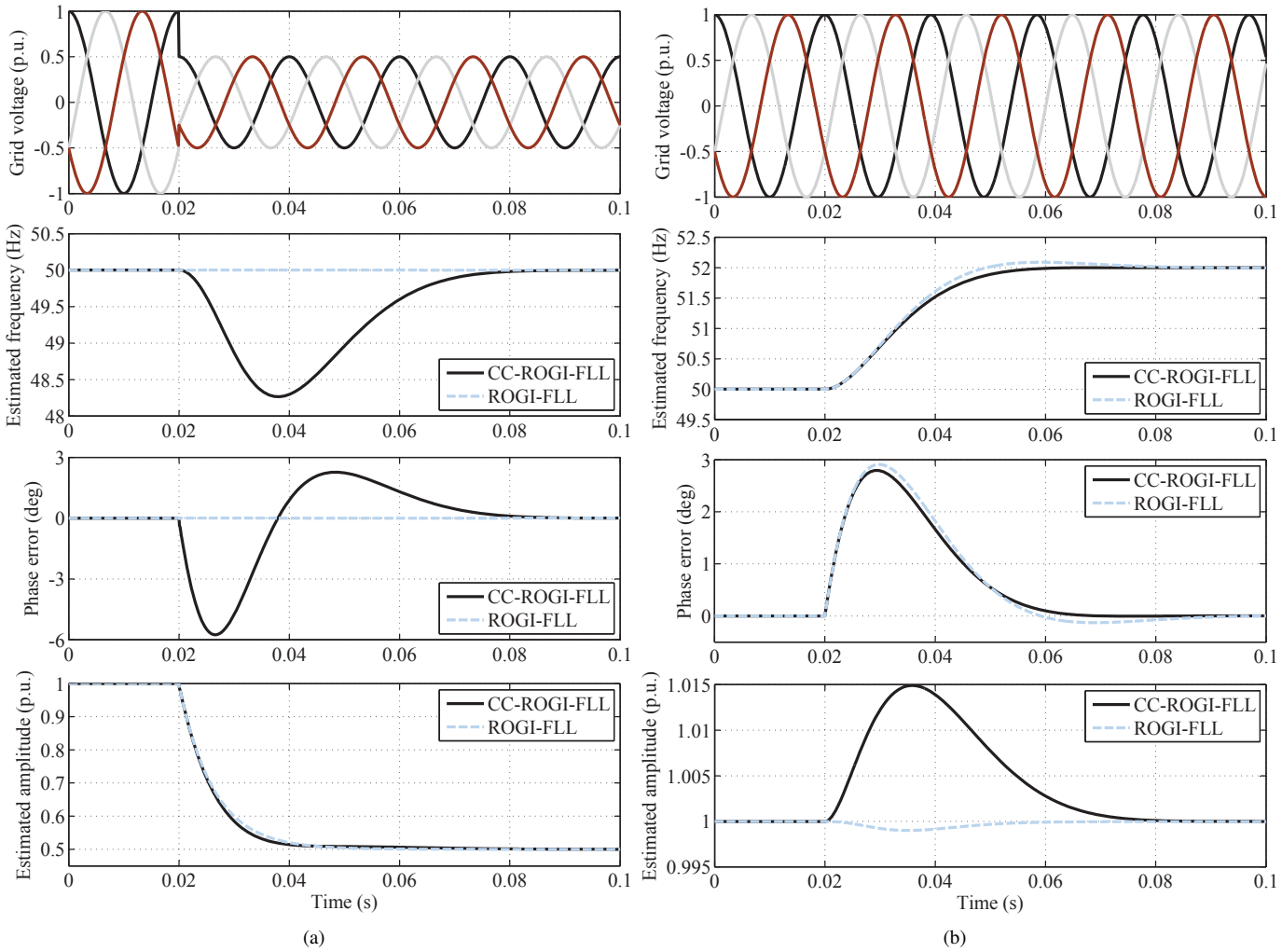

Fig. 5. Dynamic performance comparison between the CC-ROGI-FLL and ROGI-FLL. (a) 0.5 p.u. voltage sag. (b) +2 Hz frequency jump. ROGI-FLL parameters: $k = 160$ and $\lambda = 12791$ [4]. CC-ROGI-FLL parameters: $k = 160$, $k' = -64$, and $\lambda = 12791$.

III. Drawbacks of CC-ROGI-FLL

A. Creating Coupling Between Control Loops

In Section II, a small-signal model for the CC-ROGI-FLL was derived. According to this model and that of the standard ROGI-FLL, which is shown in Fig. 3(b) [4], the following observations can be made.

- In the small-signal model of the ROGI-FLL, there is no coupling between the phase/frequency and amplitude estimations loops. It implies that, from the large-signal point of view, there is a very weak coupling between these loops. Therefore, for example, an amplitude jump in the three-phase input signals of the ROGI-FLL has a negligible influence on estimating the grid voltage phase and frequency. Similarly, a frequency jump in the grid voltage barely affects the estimated amplitude by the ROGI-FLL. The dashed lines in Fig. 5 demonstrate these facts.
- In the CC-ROGI-FLL model, however, there is a cross-coupling between the amplitude and phase/frequency estimations loops, which is a direct result of using a complex control gain. The coupling level is proportional to k'. Therefore, depending on the value of k', large spurious transients in the CC-ROGI-FLL performance may happen. The solid lines in Fig. 5 demonstrate this drawback of the CC-ROGI-FLL. Table I summarizes details of these simulation results. The description of the numerical tests and the FLLs control parameters[2] may be found in the caption of Fig. 5.

B. Increased Complexity in Tuning and Analysis

The coupling between the amplitude and phase/frequency estimations loops of the CC-ROGI-FLL, regardless of the aforementioned spurious transients, makes its stability analysis and tuning its control parameters more complicated compared to the standard ROGI-FLL. Notice that for the stability analysis and tuning of the CC-ROGI-FLL, we have to obtain the matrices of its open-loop and closed-loop transfer functions from its small-signal model and apply multi-input-multi-output

[2]To have a fair comparison, the values of k and λ in the CC-ROGI-FLL are the same as those in the ROGI-FLL. The value of k' in the CC-ROGI-FLL is set equal to -64. It is the minimum possible value that removes the overshoot in the estimated frequency of the CC-ROGI-FLL in response to a frequency jump for the selected values of k and λ.

TABLE I
DETAILS OF SIMULATION RESULTS

	CC-ROGI-FLL	ROGI-FLL
Test 1: Voltage sag		
5% Settling time	16.4 ms	18.7 ms
Amplitude overshoot	0%	0%
Peak frequency variation	1.74 Hz	0 Hz
Peak phase variation	5.8°	0°
Test 2: Frequency jump		
5% Settling time*	30.7 ms	25.9 ms
Frequency overshoot	0%	4.4%
Peak phase variation	2.8°	2.9°
Peak amplitude variation	0.015 p.u.	0.001 p.u.

* If the 2% threshold is considered, the settling time of the CC-ROGI-FLL in this test will be shorter than that of the ROGI-FLL.

(MIMO) control tools. These tools are more complicated than single-input-single-output (SISO) ones, which are applicable to the ROGI-FLL.

C. Amplifying Frequency Components Around Fundamental Frequency

By assuming that the estimated frequency $\hat{\omega}$ is a constant, the transfer functions relating the extracted fundamental component by the ROGI-FLL [Fig. 1] and CC-ROGI-FLL [Fig. 2] to their inputs can be expressed in the space vector notation as

$$G_{\mathrm{ROGI-FLL}}(s) = \frac{\hat{v}_{\alpha,1}(s) + j\hat{v}_{\beta,1}(s)}{v_\alpha(s) + jv_\beta(s)} = \frac{k}{(s - j\hat{\omega}) + k} \quad (20)$$

$$G_{\mathrm{CC-ROGI-FLL}}(s) = \frac{\hat{v}_{\alpha,1}(s) + j\hat{v}_{\beta,1}(s)}{v_\alpha(s) + jv_\beta(s)} = \frac{k + jk'}{(s - j\hat{\omega}) + k + jk'}. \quad (21)$$

The Bode magnitude plots of these transfer functions can be observed in Fig. 6. Both these transfer functions have a unity gain at the fundamental frequency, which means they correctly extract the grid voltage fundamental component. The CC-ROGI-FLL, however, amplifies a frequency range in the neighborhood of the fundamental frequency. This amplification results in larger oscillatory errors in the estimated quantities by the CC-ROGI-FLL compared to the ROGI-FLL if the grid voltage contains a disturbance component in that frequency range. Notice that the aforementioned frequency range spans from $\hat{\omega}$ to $\hat{\omega} - 2k'$, and the maximum amplification gain in this range is equal to $\sqrt{1 + (k'/k)^2}$. Therefore, to minimize this problem, k' should be as small as possible.

IV. CONCLUSION

In this work, further investigations on a recently proposed idea (i.e., using a complex control gain in three-phase FLLs) were conducted. To this end, a standard ROGI-FLL with a complex control gain, briefly called the CC-ROGI-FLL, was considered and a small-signal model for that was derived. The model shows that a complex control gain results in a coupling between the amplitude and phase/frequency estimation loops. The coupling level is proportional to the value of k' (i.e., the imaginary part of the complex control gain). It was shown

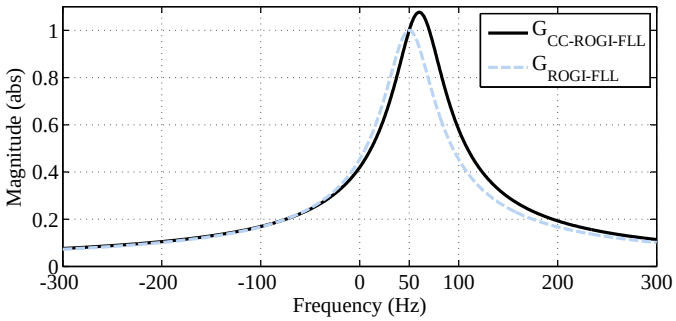

Fig. 6. Bode magnitude plots of (20) and (21). Parameters: $k = 160$, $k' = -64$, and $\hat{\omega} = 2\pi 50$ rad/s.

using numerical results that this coupling may cause large spurious transients in estimating the grid voltage parameters. It was also demonstrated using Bode magnitude plots that using a complex control gain amplifies components within a frequency range in the neighborhood of the fundamental frequency. This amplification is proportional to k'. Therefore, depending on the value of k', it may cause large oscillatory errors in the CC-ROGI-FLL estimated parameters if the grid voltage contains a harmonic/inter-harmonic in that frequency range. It was also briefly discussed that using a complex control gain makes the analysis and tuning of the FLL more difficult as MIMO control design tools need to be applied.

All these negative aspects suggest that a very careful attention should be paid to the application of a complex control gain in three-phase FLLs. It is also recommended in this work to keep the absolute value of imaginary part of the complex control gain as small as possible if the application of such a gain is intended.

REFERENCES

[1] X. Q. Guo and W. Y. Wu, "Simple synchronisation technique for three-phase grid-connected distributed generation systems," *IET Renew. Power Gen.*, vol. 7, no. 1, pp. 55–62, Feb. 2013.

[2] X. Q. Guo, "Frequency-adaptive voltage sequence estimation for grid synchronisation," *Electronics Letters*, vol. 46, no. 14, pp. 980–982, Jul. 2010.

[3] S. G. Jorge, C. A. Busada, and J. A. Solsona, "Frequency adaptive discrete filter for grid synchronization under distorted voltages," *IEEE Trans. Power Electron.*, vol. 27, no. 8, pp. 3584–3594, Aug. 2012.

[4] S. Golestan, J. M. Guerrero, J. Vasquez, A. M. Abusorrah, and Y. A. Al-Turki, "A study on three-phase FLLs," *IEEE Trans. Power Electron.*, pp. 1–1, 2018.

[5] E. Guest and N. Mijatovic, "Discrete-time complex bandpass filters for three-phase converter systems," *IEEE Trans. Ind. Electron.*, pp. 1–1, 2018.

[6] S. Vazquez, J. A. Sanchez, M. R. Reyes, J. I. Leon, and J. M. Carrasco, "Adaptive vectorial filter for grid synchronization of power converters under unbalanced and/or distorted grid conditions," *IEEE Trans. Ind. Electron.*, vol. 61, no. 3, pp. 1355–1367, Mar. 2014.

[7] W. Li, X. Ruan, C. Bao, D. Pan, and X. Wang, "Grid synchronization systems of three-phase grid-connected power converters: A complex-vector-filter perspective," *IEEE Trans. Ind. Electron.*, vol. 61, no. 4, pp. 1855–1870, Apr. 2014.

[8] S. Golestan, J. M. Guerrero, and J. C. Vasquez, "High-order frequency-locked loops: A critical analysis," *IEEE Trans. Power Electron.*, vol. 32, no. 5, pp. 3285–3291, May. 2017.

[9] X. Quan, X. Dou, Z. Wu, M. Hu, and A. Q. Huang, "Complex-coefficient complex-variable filter for grid synchronization based on linear quadratic regulation," *IEEE Trans. Ind. Informat.*, vol. 14, no. 5, pp. 1824–1834, May. 2018.

[10] Z. Xin, R. Zhao, F. Blaabjerg, L. Zhang, and P. C. Loh, "An improved flux observer for field-oriented control of induction motors based on dual second-order generalized integrator frequency-locked loop," *IEEE J. Emerging Sel. Top. Power Electron.*, vol. 5, no. 1, pp. 513–525, Mar. 2017.

Saeed Golestan (M'11-SM'15) received the B.Sc. degree in electrical engineering from Shahid Chamran University of Ahvaz, Iran, in 2006, the MSc degree in electrical engineering from the Amirkabir University of Technology, Tehran, Iran, in 2009, and the PhD degree in electrical engineering from Aalborg University, Aalborg, Denmark, in 2018.

He is currently an assistant professor at the Department of Energy Technology, Aalborg University, Denmark. His research interests include synchronization and signal processing techniques in power applications, and modeling and control of power converters.

Josep M. Guerrero (S'01-M'04-SM'08-FM'15) received the B.S. degree in telecommunications engineering, the M.S. degree in electronics engineering, and the Ph.D. degree in power electronics from the Technical University of Catalonia, Barcelona, Spain, in 1997, 2000, and 2003, respectively.

Since 2011, he has been a Full Professor with the Department of Energy Technology, Aalborg University, Aalborg, Denmark, where he is responsible for the Microgrid Research Program. In 2012, he was a Guest Professor with the Chinese Academy of Science and the Nanjing University of Aeronautics and Astronautics; and in 2014, he was the Chair Professor with Shandong University. His research interests include different microgrid aspects, including power electronics, distributed energy-storage systems, hierarchical and cooperative control, energy management systems, and optimization of microgrids and islanded minigrids.

Dr. Guerrero was awarded by Thomson Reuters as an ISI Highly Cited Researcher.

Juan C. Vasquez (M'12-SM'14) received the B.S. degree in electronics engineering from UAM Manizales, Manizales, Colombia, and the Ph.D. degree in automatic control, robotics, and computer vision from the Technical University of Catalonia, Barcelona, Spain, in 2004 and 2009, respectively.

In 2011, he was an Assistant Professor and from 2014 he is working as an Associate Professor with the Department of Energy Technology, Aalborg University, Denmark, where he is the Vice Programme Leader of the Microgrids Research Program. His current research interests include operation, advanced hierarchical and cooperative control, and the integration of Internet of Things into the SmartGrid.

Dr. Vasquez is an Associate Editor for IET POWER ELECTRONICS and in 2017 he was awarded by Thomson Reuters as Highly Cited Researcher. He is currently a member of the IECSEG4 on LVDC safety for use in developed and developing economies, the TC-RES in IEEE INDUSTRIAL ELECTRONICS, PELS, IAS, and PES Societies.